THE ASTROPHYSICAL JOURNAL, 401:495–507, 1992 December 20

HIGH-ENERGY PARTICLE ACCELERATION BY EXPLOSIVE ELECTROMAGNETIC INTERACTION IN AN ACCRETION DISK

C. A. HASWELL[1]
Department of Astronomy, University of Texas at Austin, Austin, TX 78712
T. TAJIMA
Department of Physics, University of Texas at Austin, Austin, TX 78712
AND
J.-I. SAKAI
Department of Applied Mathematics and Physics, Toyama University, Toyama 930, Japan
Received 1992 January 31; accepted 1992 June 24

ABSTRACT

By examining electromagnetic field evolution occurring in an accretion disk around a compact object, we arrive at an explosive mechanism of particle acceleration. Flux-freezing in the differentially rotating disk causes the seed and/or generated magnetic field to wrap up tightly, becoming highly sheared and locally predominantly azimuthal in orientation. We show how asymptotically nonlinear solutions for the electromagnetic fields may arise in isolated plasma blobs as a result of the driving of the fluid equations by the accretion flow. These fields are capable of rapidly accelerating charged particles from the disk. Our results have implications for the hard component of astrophysical jets, for accretion disk coronae, and for cosmic rays. In particular, acceleration through the present mechanism from active galactic nuclei (AGNs) can give rise to energies beyond 10^{20} eV. Such a mechanism may present an explanation for the extragalactic origin of the most energetic observed cosmic rays.

Subject headings: acceleration of particles — accretion, accretion disks — galaxies: active — MHD — radiation mechanisms: miscellaneous

1. INTRODUCTION

Accretion disks are commonly invoked in models of astronomical objects. In interacting binary stars there is an abundance of evidence for the presence of disks: double-peaked emission lines are observed; eclipses of an extended light source centered on the primary occur, and in some cases eclipses of the secondary star by the disk, are also detected. The case for the presence of disks in active galactic nuclei (AGNs) is less clear-cut; nontheless disk-fed accretion onto a supermassive black hole is the commonly accepted standard model for these objects. Observations of protostars are also indicative of disk accretion.

Jetlike phenomena are observed on a wide range of scales in accretion disk systems. The most powerful of such phenomena occur in quasi-stellar radio sources and strong radio galaxies, while there are examples of objects sharing some characteristics with these on a wide range of scales: Seyfert galaxies, SS 433, and bipolar outflows around young stars. A review of the observational properties of extragalactic jets is to be found in Bridle & Perley (1984), while Begelman, Blandford, & Rees (1984) give a thorough review of the theory of hydrodynamic phenomena in extragalactic radio jets. Margon (1984) gives a discussion of the SS 433 system. It is possible that some aspects of the fundamental physics are common to many of these and to the sprays observed in solar flares which accompany a jetlike phenomenon. The physics of the hydrodynamic flows from these objects and of their interaction with the ambient coronal, interstellar, or intergalactic matter is obviously an important subject: in the present work, however, we focus on the mechanism of the acceleration of high-energy particles, comprising a hard component of the outflow. Although the mechanism of particle acceleration in the present paper is generic, so that it may be applicable to the variety of astrophysical objects which exhibit strong differential rotation with a magnetized disk, the most dramatic implications of the present paper concern cosmic-ray production by AGNs. The highest energy particles obtained from acceleration in AGNs is of obvious importance to cosmic-ray physics, so we will focus on this subject in the discussion § 6.

In this paper we consider magnetic accretion disks. We examine the MHD evolution of the magnetic fields in a differentially rotating disk and the consequences of such field evolution. Specifically we show that explosive (that is to say very rapidly growing—more precise definition given later) solutions arise for the electromagnetic fields and that these fields lead to rapid acceleration and ejection of relativistic charged particles. The growth of the electromagnetic fields is indirectly driven by the gravitational energy manifest in the accretion flow. Some small fraction of the energy embodied in the bursting fields is converted into kinetic energy of ejected particles; the majority of the energy is thermally dissipated in the local plasma.

Consider then a compact object accreting material from an accretion disk. We assume the existence of a seed magnetic field in the disk. This seed field could be due to the ambient interstellar or intergalactic field, or alternatively, could be either a zeroth order representation of a dipole field due to the central object, or the asymptotic field resulting from relaxation of strained fields sheared by the disk matter motion. Since the material in the disk is expected to be fairly highly ionized, it is argued that flux-freezing of the seed magnetic field in the diferentially rotating plasma occurs. So long as the fields are

[1] Current address: Space Telescope Science Institute, 3700 San Martin Drive, Baltimore, MD 21218.

confined by the disk, this causes the magnetic field to wrap up tightly, becoming highly sheared and predominantly azimuthal in orientation: a manifestation of the dynamo effect elucidated by Parker (1970). A magnetohydrodynamic (MHD) computation of the interaction of a Keplerian accretion disk with an initially uniform magnetic field in the plane of the disk was performed by Tajima & Gilden (1987), although the configuration of their fields is by no means a unique choice. As illustrated in Figure 1*a*, the field in the disk was found to adopt a banded structure: bands of tightly wrapped azimuthal field lines, with reversals in field direction, interspersed with less dense bands. The field lines became progressively more tightly wrapped until reconnection took place, resulting in a more relaxed topology. Subsequently wrap-up proceeded again and the sequence recurred periodically. The development of this type of structure in a differentially rotating disk was essentially independent of the initial conditions used in this two-dimensional computation. The MHD dynamics out of the plane of the disk, such as the magnetic buoyancy, have also been studied (Shibata, Tajima, & Matsumoto 1990). This study finds additional phenomena but leads to no conclusion inconsistent with the results of the in-plane simulation.

Sofue, Fujimoto, & Wielebinski (1986) present a study of the three-dimensional magnetic field structure in a galactic disk. The resulting calculations are elucidated in Sawa & Fujimoto (1986) and Fujimoto & Sawa (1987). Again the field embedded within the disk shows a tightly wrapped azimuthal structure with many reversals in direction. This configuration includes many closed loops above the plane of the disk. These loops are anchored in the disk plane, and in reality the loops would be broken as a result of the differential rotation in the disk, similar to the results of Shibata et al. (1990). This would then lead to open antiparallel poloidal fields in the coronal plasma. In what follows we consider the fields in the disk only.

If the disk is subject to shear flow or buoyancy instabilities, the wrap-up of the magnetic field, which is the basis of the calculations reviewed above, could be inhibited or mitigated. The mixing caused by these instabilities mitigates the field growth for two reasons: first, the flow is no longer purely azimuthal, so the dynamo effect is weakened; second, as mixing occurs across a field reversal, magnetic reconnection will occur, dissipating the azimuthal field. As a result of this, if the condition for instability is fulfilled at a given instant, the result will be a subsequent weakening of the magnetic field. Therefore in accretion disks which are globally unstable, we expect the magnetic fields to be modest. Such disks will not undergo the explosive evolution we will explore in this paper. Shibata et al. (1990) present discussion of two types of disks: those which are "magnetically cataclysmic" and those which are not. In this paper we are concerned with magnetically catalysmic disks.

In the MHD analysis presented in § 2 and § 3 we follow the evolution of an element of plasma as it encounters the boundary layer near the inner edge of the accretion disk. At the boundary layer the radial (accretion) velocity v_r of the element may become appreciable. We take the initial magnetic field to be essentially azimuthal in orientation and tightly wrapped with reversals in field direction, like the structure in the dense bands of the Tajima-Gilden computation. A computation of a magnetic plasma with differential shearing motion imposed upon it was performed in a study of the dynamic evolution of coronal loops (Steinolfson & Tajima 1987). Their configuration, however, had an aspect ratio (h/r) quite different to that of the accretion disk currently under consideration; and a differential rotation was continually applied at the two footpoints. The results indicated the development of considerable currents along the axis, which induced spiraling magnetic fields that pinched the plasma. These spiraling fields were originally nearly force-free and often exhibited complicated geometries such as field reversal; however, in later stages the azimuthal field increased explosively. The word "explosive" means that the temporal growth is much faster than the exponential

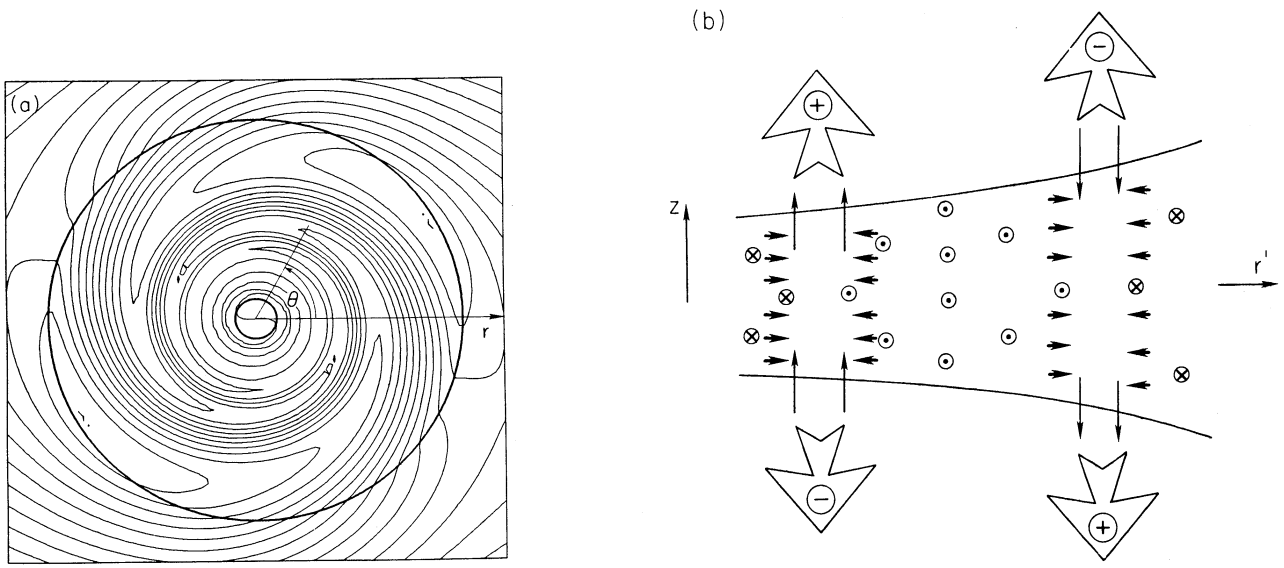

FIG. 1.—Cartoon depictions of the magnetic field topology. (*a*) The structure found in the Tajima-Gilden MHD simulations. The magnetic field is predominantly azimuthal, exhibiting a banded structure with many reversals in magnetic field direction. (*b*) A cross section of a portion of the inner disk showing two adjacent magnetic reversals. This cartoon illustrates the magnetic collapse process explored in this paper. The magnetic field direction is indicated with the standard symbols. The small, dark arrows show the direction of the bulk MHD fluid flow; the long thin arrows show the electric field vectors, and the larger, unfilled arrows indicate the direction of ejection of charged particles which decouple from the MHD flow.

growth; the explosive growth (if continued) reaches infinity with a finite time, while the exponential one takes infinite time to reach infinity. The explosive process can also be driven by the accretion flow (Keplerian motion in the case of a thin disk) of the disk under consideration: in § 3 we show how explosive solutions arise from the equations governing the electromagnetic fields. Such solutions are characteristic of highly nonlinear, driven plasma processes which are expected to occur in the accretion disk boundary layer plasma in question. The azimuthal magnetic field within an element of accreting plasma increases extremely rapidly, and likewise decays, with Faraday induction simultaneously causing correspondingly increasing electric fields. Once this occurs, the electromagnetic field configuration is capable of rapidly accelerating some of the disk particles; this is discussed in § 4. Numerical work in which trajectories of accelerated particles are calculated is presented in § 5; in § 6 we discuss our results, and their implications, in particular to ultra–high-energy cosmic rays.

2. OUR MODEL AND BASIC EQUATIONS

We consider field evolution driven by the (MHD) fluid dynamics in the disk. The particle acceleration in our model arises as a result of electromagnetic field evolution. Our starting equations are the Euler equation and the magnetic induction equation.

In the magnetic field configuration we introduced in § 1, magnetic field compression and reconnection take place periodically as a result of the differentially rotating fluid and the highly sheared, predominantly azimuthal magnetic field (Tajima & Gilden 1987). The regeneration or sustenance of the magnetic field due to the dynamo effect occurs continuously. We focus on the behavior of elements of plasma at or near the inner edge of the accretion disk, where the accretion of matter permeated with magnetic field onto the compact object helps to drive the enhancement of the magnetic field. A cartoon of the resulting magnetic collapse and reconnection events, and the consequent particle acceleration, is presented in Figure 1*b*.

In order to separate the effects due to the steady-state rotational velocity, we transform to a rotating frame of reference, chosen to be rotating with the steady angular velocity of the blob of plasma under scrutiny. We denote this particular value with the symbol $\boldsymbol{\Omega}$; $\boldsymbol{v}_0$ is the velocity of the rotating frame, and $\boldsymbol{u}$ is the velocity with respect to the rotating frame, i.e. at the radius of interest, $\boldsymbol{u}$ is the deviation from the equilibrium motion. The electromagnetic fields and current transform according to the Lorentz transform, and Ohm's law provides a relationship between $\boldsymbol{E}$ and $\boldsymbol{B}$. For simplicity we restrict our MHD analysis to the nonrelativistic regime, and neglect terms of order u/c or v_0/c. Since $\boldsymbol{v}_0$ is azimuthal and $\boldsymbol{B}$ is predominantly azimuthal, $\boldsymbol{v}_0 \times \boldsymbol{B}$ is very small compared to $\nabla \times \boldsymbol{B}$, and may therefore be neglected. Assuming that the plasma is highly conducting, the resistivity, η, is small. The details of the transformation of frames are given in Appendix A. The induction equation in the rotating frame of reference is then

$$\frac{\partial \boldsymbol{B}}{\partial t} + \boldsymbol{\Omega} \times \boldsymbol{B} - \nabla \times \boldsymbol{u} \times \boldsymbol{B} = \frac{c^2 \eta}{4\pi} \nabla^2 \boldsymbol{B}\,, \tag{1}$$

and the Euler equation in the rotating frame is

$$\frac{\partial \boldsymbol{u}}{\partial t} + 2\boldsymbol{\Omega} \times \boldsymbol{u} + (\boldsymbol{u} \cdot \nabla)\boldsymbol{u} = \frac{c}{4\pi} (\nabla \times \boldsymbol{B}) \times \boldsymbol{B} + \eta_{\rm vis} \nabla^2 \boldsymbol{u}\,, \tag{2}$$

where $\eta_{\rm vis}$ is the coefficient of viscosity. Equations (1) and (2) do not carry explicit gravitational terms, though there is an indirect dependence on gravity through the angular velocity $\boldsymbol{\Omega}$. In the sense that $\boldsymbol{u}$ is the deviation from the steady state rotational velocity at the radius of interest, these equations are local: they are correct everywhere in the disk, but at other radii $\boldsymbol{u}$ and $\boldsymbol{\Omega}$ have no special physical significance. We now adopt the approximation that the disk is axisymmetric; as a result, the visosity will not enter into our nonlinear analysis, though the viscosity plays a crucial role in determining the nature of the accretion flow, and hence is indirectly responsible for the magnetic field buildup which triggers the behavior we will examine. In Appendix B we discuss a relationship between the viscosity and the resistivity in a highly turbulent magnetic plasma.

3. NONLINEAR EXPLOSIVE PROCESSES

We present here a simplified heuristic derivation of the explosive evolution of the electromagnetic fields. The word explosive is used both technically (see for example, Tajima et al. 1987) and figuratively. The technical definition of the explosive growth is that the quantity grows faster than exponentially in time so that it could increase toward infinity in a finite time: an example of an explosive quantity is the expression $(t_0 - t)^{-\alpha}$, with $\alpha > 0$. Here, and subsequently, t_0 is a constant. The purpose of this discussion is to illuminate the basic physical processes at work here; the results of a more complete treatment will be given at the end of this section.

We are interested in the azimuthal component of the magnetic field. This is coupled with the radial component of the velocity. Therefore we examine the radial component of Euler's equation and the azimuthal component of the induction equation:

$$\frac{\partial u_r}{\partial t} + \frac{u_r}{r}\frac{\partial}{\partial r}(r u_r) - 2\Omega u_\theta = \frac{c}{4\pi}\frac{1}{r}\frac{\partial}{\partial r}(r B_\theta) B_\theta + \eta_{\rm vis}\left(\frac{1}{r^2}\frac{\partial}{\partial r} r^2 \frac{\partial u_r}{\partial r} - \frac{2u_r}{r^2}\right), \tag{3}$$

$$\frac{\partial B_\theta}{\partial t} + \Omega B_r - \frac{\partial}{\partial r}(u_r B_\theta - u_\theta B_r) = -\frac{c^2 \eta}{4\pi}\frac{\partial}{\partial r}\left[\frac{1}{r}\frac{\partial}{\partial r}(r B_\theta)\right]. \tag{4}$$

If we assume that $u_\theta = B_r = 0$ at $t = 0$, then the above two equations are closed by themselves. In general, the linear terms may be important and the azimuthal velocity and radial magnetic field are coupled into the evolution of the terms of interest; however, we contend that the azimuthal magnetic field is likely to be dominant in equations (3) and (4), since this component of the magnetic field is stretched and enhanced by the differential rotation in the disk (the dynamo effect).

The results of Kaisig & Spruit (1991) show that thin disks with high Reynolds numbers are stable against turbulence. With this in mind, our magnetic fields may be viewed as a global structure set up by the wrapping up of field lines in a nonturbulent differentially rotating disk. The wrapping causes the azimuthal field to become intense. The field growth is offset by dissipation caused by the finite conductivity of the plasma, and in the steady state disk magnetic reconnection occurs. In an element of plasma encountering the boundary layer at the inner edge of the disk, however, nonlinear behavior could occur over the magnetic evolution time scale. At the inner edge of the disk the extreme energies involved in the accretion process are available to drive the field evolution.

As a result of turbulent fluctuations in the region of the

boundary layer, the nonlinear terms may become dominant over the linear terms in localized elements of plasma. By nonlinear we mean terms which are quadratic in the variables u_r and B_θ. Once the nonlinear terms become dominant over the linear terms (the latter being the Coriolis term, ΩB_r, and the resistive term), then we may drop the linear terms in favor of the nonlinear terms. The regime where this is justified could be termed the asymptotically nonlinear regime. Such treatment is valid only in the local temporal and spatial neighborhood of the strongly driven magnetic fields. In the following we will not be discussing global field evolution. To satisfy the prerequisites of an asymptotically nonlinear treatment, we require

$$2\Omega u_\theta \ll \frac{u_r}{r}\frac{\partial}{\partial r}(ru_r)\,, \tag{5}$$

and

$$\Omega B_r \ll u_r k_r B_\theta\,, \tag{6}$$

where k_r is the scale length of radial variations of $u_r B_\theta$. Whenever these inequalities are satisfied as a result of a fluctuation in the velocity and magnetic field structure of a plasma element, we may simplify equations (3) and (4) to

$$\frac{\partial u_r}{\partial t} = -\frac{u_r}{r}\frac{\partial}{\partial r}(ru_r) + \frac{c}{4\pi}\frac{1}{r}\frac{\partial}{\partial r}(rB_\theta)B_\theta\,, \tag{7}$$

$$\frac{\partial B_\theta}{\partial t} = \frac{\partial}{\partial r}(u_r B_\theta - u_\theta B_r)\,. \tag{8}$$

These equations, along with the continuity equation (Tajima et al. 1987), have the structure of quadratic nonlinearity on the right-hand side, equated to the time evolution terms on the left-hand side. For illustration let us consider equations (7) and (8) alone, which admit solutions of the form

$$B_\theta \sim \frac{B_0(x)}{(t_0 - t)}\,, \tag{9}$$

$$u_r \sim \frac{u_0(x)}{(t_0 - t)}\,, \tag{10}$$

where B_0 and u_0 are constants. It goes without saying that such solutions are valid only when the nonlinearities are sufficiently strong to justify the treatment outlined above, and when t is not too close to t_0. The latter condition arises when the nonlinear fields become so strong that physical effects which were negligible at the onset become important: we return to discuss this point in § 4. If the continuity equation is taken into account, it can play a role in stopping the explosive process from diverging to infinity. Furthermore, as we shall see at the end of this section, if one includes the continuity equation in one-dimensional fashion, one can derive explosive solutions similar to equations (9) and (10) with a slightly modified exponent to $(t_0 - t)$ (Tajima et al. 1987).

It could be argued that magnetic buoyancy effects will tend to disperse the growing field represented by equation (9). We may counter this argument with two observations: first, even after the Parker instability in the disk proceeds to the nonlinear phase of its evolution, there is still a substantial amount of flux remaining embedded in the central part of the disk (Shibata et al. 1990); and more importantly, once the explosive process begins, its time scale is far too fast for buoyancy forces to have an appreciable effect on the magnetic field configuration.

From the radial component of Faraday's law we have $\partial B_r/\partial t = \Omega B_\theta$. Hence the solutions given by equations (9) and (10) are close to the true solutions in the highly nonlinear regime, and we can use them to iluminate such explosive evolution. There is no dependence on Ω in equations (9) and (10): the differential rotation in the disk is unimportant in influencing the character of the nonlinear evolution once this regime is entered. The importance of the differential flow is in providing the initial magnetic field buildup through the sheared velocity field. Without such buildup of magnetic field energy and continual driving from the energy in the accretion flow, the explosive evolution would not be possible.

Now we will examine the consequences of these highly nonlinear solutions for the magnetic field evolution. First we consider the response of the electric field E_z to the growth in B_θ. The azimuthal component of the induction equation is

$$\frac{\partial B_\theta}{\partial t} = c\frac{\partial E_z}{\partial r}\,; \tag{11}$$

hence substituting from equation (9) for B_θ, $B_0/(t_0 - t)^2 = c(\partial E_z/\partial r)$. From this we can see that E_z consists of a curl-free part and a part which varies temporally as

$$\frac{B_0}{(t_0 - t)^2}\,. \tag{12}$$

Away from the magnetic field null point (the null point is at the reversal), the induced electric field is nothing but the manifestation of the radial flow of the fluid, which in the final analysis is driven by the gravitational force; locally it could be said to be driven by the fluid velocity described in equation (10).

We have shown how the feedback between the magnetic induction equation and Euler's equation can lead to explosively growing electromagnetic fields in an element of the disk plasma. We have not, however, derived a complete solution: we have not considered the spatial dependences, and we have ignored the continuity equation.

In order to obtain a complete solution for the exploding fields, a lengthier algebraic treatment is required; this treatment is elaborated in Tajima & Sakai (1989a, b), and in Tajima et al. (1987). Since our purpose here is to explore the consequences of the explosive magnetic buildup in an accretion disk, we refer the interested reader to the original papers for details of the derivation and include below only sufficient detail to make the coordinate frame and notation clear.

We retain our focus on a single element of plasma in which is situated a magnetic field reversal. In the following discussion we will employ modified cylindrical coordinates in which r denotes the radial coordinate in a local frame of reference, the zero being located at the radius of the field reversal itself, i.e., r does not represent the radial distance from the center of the compact object. We will use R_0 for the radial distance of the zero point of r from the center of the compact object, so

$$r = r' - R_0\,, \tag{13}$$

where r' is the conventional radial coordinate in a cylindrical coordinate system.

The analysis presented by Tajima et al. (1987) begins with the assumption that the magnetic field B_θ can be represented by

$$B_\theta = B_0\frac{r}{\lambda}\,, \tag{14}$$

where λ is the thickness of the current sheet at the magnetic field reversal. This dependence is a simple approximation to the true dependence: since the field is tightly wrapped the configuration will be almost axisymmetric; $B_\theta(r)$ will be essentially antisymmetric around the reversal, and the linear dependence is an approximation to the true function, valid in the region close to the reversal. The analysis leads to self-consistent solutions for the electromagnetic fields in the explosive phase given by

$$E_r = -\frac{2}{9}\frac{m_i}{e}\frac{r}{(t_0 - t)^2}, \tag{15}$$

$$B_\theta = \left(\frac{2}{9}\right)^{2/3}\frac{B_{00}\lambda^{1/3}r}{V_A^{4/3}(t_0 - t)^{4/3}}, \tag{16}$$

$$E_z = \frac{2}{3}\left(\frac{2}{9}\right)^{2/3}\frac{B_{00}\lambda^{1/3}r^2}{V_A^{4/3}c(t_0 - t)^{7/3}} + \frac{2}{3}\left(\frac{2}{9}\right)^{1/3}\frac{B_{00}c}{\omega_{pe}^2\lambda^{1/3}V_A^{2/3}(t_0 - t)^{5/3}}, \tag{17}$$

where

$$V_A = \frac{B_{00}}{\sqrt{4\pi\rho}},$$

m_i is the ion mass, B_{00} is a constant, and ω_{pe} is the electron plasma frequency. Note that the most rapidly growing term is the first term in the expression for E_z.

The explosive electromagnetic field gives rise to the MHD $\boldsymbol{E} \times \boldsymbol{B}$ motion (bulk fluid motion) causing plasma on both sides of the reversal to flow toward the field null point. The physical phenomenon described in the field solutions is self-driving. The current sheet at the field reversal induces the growing magnetic fields; the growth of the fields causes compression which pinches the current sheet.

The growing fields are dictated by the form of equations (7) and (8). The solutions embodied in equations (15)–(17) are scale-free: neither the temporal nor the spatial scale has been quantitatitvely fixed by our arguments. We require merely that the spatial scale be small compared with the field reversal scale itself, and that the characteristic time scale of the explosive processes be sufficiently short to prevent buoyancy forces from removing the generated field. The radial size of the present magnetic structure, L_B, is related to the spatial scale of the current sheet, λ, through the magnetic Reynolds number, R_m. The magnetic Reynolds number is defined as the ratio of the resistive time scale, $\tau_{\rm res}$, to the dynamical time scale, $\tau_{\rm dyn}$, i.e.,

$$R_m \sim \frac{|\nabla \times (\boldsymbol{u} \times \boldsymbol{B})|}{|\eta\nabla^2\boldsymbol{B}|}; \tag{18}$$

R_m is a fundamental dimensionless plasma parameter. The expression in the numerator of equation (18) consists of four terms

$$B_\theta\frac{1}{r}\frac{\partial u}{\partial\theta};\quad B_r\frac{\partial u}{\partial r};\quad u_r\frac{\partial B}{\partial r};\quad u_\theta\frac{1}{r}\frac{\partial B}{\partial\theta}. \tag{19}$$

Since $\boldsymbol{B}$ and $\boldsymbol{u}$ are both predominantly azimuthal, and both have larger radial gradients than azimuthal gradients, all these terms are probably of approximately the same order. Choosing the last of these terms as representative and performing dimensional analysis yields

$$R_m \sim \frac{u_\theta L_B^2}{\eta R}. \tag{20}$$

Here R is the scale of variations of $\boldsymbol{B}$ in the azimuthal direction, which could be visualized as the "wrap length" between magnetic field reversals. The sheet current width, λ, is determined by the balance of diffusion of the magnetic field and rotational regeneration. Thus the spatial scale, λ, is obtained from dimensional analysis of

$$\nabla \times (\boldsymbol{u} \times \boldsymbol{B}) \sim \eta\nabla^2\boldsymbol{B}, \tag{21}$$

where the spatial derivative on the left-hand side is over wrap length, while the one on the right-hand side is over the current sheet. From equation (21) we obtain

$$\lambda \sim \sqrt{\frac{\eta R}{u_\theta}}. \tag{22}$$

Hence with equation (20)

$$\lambda \sim \frac{L_B}{\sqrt{R_m}}. \tag{23}$$

Note that the form of the dependence on R_m in equation (23) is similar to that found in Perkins & Zweibel (1987).

The stage at which our approximation breaks down can depend on both the temporal and the spatial scale. For relatively slow, large-scale bursts, the energy embodied in the field may be limited by the gravitational energy, the limiting magnetic field, $B_{\rm collapse}$, being given by

$$\frac{B_{\rm collapse}^2}{8\pi} \sim \frac{GM\rho L_B}{R_0^2}. \tag{24}$$

Here M is the mass of the compact object and ρ is the ambient mass density in the disk. This limit arises in the following way: once the magnetic field strength becomes strong enough to compress the disk plasma sufficiently that regions of reversed magnetic field are brought into contact, then reconnection will occur. In order to compress the plasma, the magnetic field will have to do work against the gravitational force. Rearranging equation (24) we obtain

$$B_{\rm collapse} \sim c\sqrt{4\pi\rho}\left(\frac{r_S}{R_0}\right)\left(\frac{L_B}{r_S}\right)^{1/2}, \tag{25}$$

where r_S is the Schwarzschild radius.

Obviously the explosive growth eventually leads to a breakdown of the assumptions used to derive equations (7) and (8). Compression of the plasma will cause increased pressure; the pressure could then inhibit the pinching caused by the growing magnetic field, and our approximation breaks down. The explosive evolution then ceases. Another possibility is a fast instability in which the field topology changes: for instance, magnetic field may peel off into the coronal region.

The explosive process recurs repetitively: the magnetic field is being continually wound up, leading to the regions of "runaway" growth in which the fields grow according to equations (15), (16), and (17); each of these bursts is ultimately terminated by magnetic reconnection across the field reversal, leading to a locally more relaxed magnetic topology. Interesting phenomena such as particle acceleration take place in plasma elements undergoing this electromagnetic evolution. In

the remainder of this paper we will examine the consequences of such cataclysmic field evolution.

When magnetic reconnection occurs across the field reversal, the energy built up in the electromagnetic fields will be released into the disk/boundary layer plasma (only a small part of this energy is expended in accelerating charged particles, since a relatively small number of particles is involved.) This energy is entrained in the kinetic energy in the compressive bulk flow toward the reversal at the moment of reconnection, and ultimately causes heating of the local disk plasma. The release and subsequent radiation of this energy may explain the flickering observed in the light curves of interacting binary systems containing accretion disks. For an example of this behavior in the cataclysmic variable HT Cas, see Horne, Wood, & Stiening (1991).

4. ACCELERATION OF PARTICLES

The plasma element under consideration is at a distance R_0 from the compact object and is centered on a field reversal. The extent of the region of interest is approximately given by $-L_B/2 \leq r \leq L_B/2$, where L_B is the radial distance over which the approximation (14) for the azimuthal magnetic field is valid. We proceed to examine how the explosively evolving fields affect the particles of the disk plasma.

Away from the field null point, the electric and magnetic fields will produce bulk flow toward the null point. It is important to notice that in the region close to the field null point, however, the MHD approximation breaks down as noted in § 3; in this region the electric fields can directly accelerate particles from the dense regions close to the central plane of the disk. There are also particles in the low-density regions at the surface of the disk, or the base of the accretion disk corona, which can be decoupled from the fluid flow in the disk and may respond directly to the electric field's evolution. Since the electric field during the "burst" phase increases much faster that the magnetic field (compare the exponents of $t_0 - t$ in eqs. [16] and [17]), the acceleration during the more extreme phases of the field evolution is expected to be increasingly in the axial direction. In addition to this explosive acceleration, magnetic acceleration, sometimes called $\boldsymbol{v}_p \times \boldsymbol{B}$ acceleration, could take place regardless of the position of the particle with respect to the field null point, as long as the particle travels with the accreting magnetic field structure (for details of this see Sakai & Ohsawa 1987).

As the cartoon in Figure 1*b* shows, in a single explosive event positively and negatively charged particles will be accelerated in opposite directions, the direction for each depending on the sense of the magnetic field reversal (clockwise B_θ to anticlockwise, or vice versa). However, the nonlinear evolution will take place in equal numbers of reversals of each sense so there will be no overall charge separation as a result of this process.

Equations of motion for a particle of mass m, charge q, and angular momentum L, at the inner edge of the disk performing near-Keplerian motion, under the influence of gravitational attraction and the electromagnetic fields discussed above are

$$\dot{p}_r = \frac{mGM(R_0 + r)}{[(R_0 + r)^2 + z^2]^{3/2}} + \frac{L^2}{(R_0 + r)^3} - \frac{qB_\theta p_z}{(m^2c^2 + p^2)^{1/2}} + qE_r , \tag{26}$$

$$\dot{p}_z = -\frac{mGMz}{[(R_0 + r)^2 + z^2]^{3/2}} + \frac{qB_\theta p_r}{(m^2c^2 + p^2)^{1/2}} + qE_z , \tag{27}$$

where z is the axial coordinate, and p_r and p_z are the radial and axial momenta.

Once a particle decouples from the fluid motion, it will be ballistically accelerated by the bursting fluids until it leaves the region of explosive evolution, or until the explosive growth subsides. The momentum attained by an accelerated particle depends on the intensity of the electromagnetic burst, and on both the time and location at which it decouples from the fluid motion. Unfortunately we are unable to quantitatively constrain the burst characteristics, and an estimate of the relative probabilities of decoupling from the MHD flow is beyond the scope of this paper. In order to make the solution tractable, our model has dropped many aspects of the physics; this means that we are unable to deduce the spectrum of particle energies which are produced by this mechanism. Clearly, however, the more energetic bursts will give rise to a higher average energy for the ejected particles. Furthermore, we are able to make an estimate of the upper limit to the energy imparted to our accelerated particles. In the most extreme cases, E_z dominates, and the particle energy, W, is given approximately by

$$W = qE_z \Delta z ,$$
$$W \approx qE_z c \Delta t , \tag{28}$$

where Δz is the axial distance the particle travels while being ballistically accelerated, and we have made the approximation that the particle velocity $\boldsymbol{v}$, has a magnitude approximately equal to c; and the trajectory is predominantly axial. For the most extreme accelerations, these approximations are fairly valid, but they break down for most cases, in which the particles are not well-collimated along the axial direction. Using equations (17) and (28) we obtain

$$W \approx q\left(\frac{2}{3}\right)\left(\frac{2}{9}\right)^{2/3} \frac{\lambda^{1/3} r^2 B_{00}}{V_A^{4/3} \Delta t_{\text{switch}}^{4/3}} . \tag{29}$$

The magnetic collapse determines the values of Δt_{switch}, the value of $(t_0 - t)$ at which the explosive acceleration ceases. In order to make numerical estimates of Δt_{swtich}, much advancement of accretion disk theory is required. Here we are particularly interested in obtaining the upper limits to the particle energy imparted by the present mechanism. In the most violent of disks or near the violent boundary layer of such disks we crudely estimate the size of the magnetic structure, L_B, to be of the order of the Schwarzschild radius, r_S; an estimate likely to lead to an overestimate of energies. When $L_B \sim R_0 \sim r_S$,

$$\Delta t_{\text{switch}}^{-4/3} \sim \frac{c\sqrt{4\pi\rho} V_A^{4/3}}{B_{00} \lambda^{1/3} r_S} \left(\frac{9}{2}\right)^{2/3} ;$$

so

$$W \sim \frac{2}{3} cq \frac{B_{00}}{V_A} r_S ,$$
$$W \sim \frac{2}{3} cqr_S \sqrt{4\pi\rho} . \tag{30}$$

Evaluating this expression for an electron or proton in terms of the particle density, n, we obtain

$$W \sim 3\left(\frac{M}{M_\odot}\right)\left(\frac{n}{10^{16}}\right)^{1/2} \text{TeV} . \tag{31}$$

TABLE 1

PARAMETERS OF NUMERICAL TRAJECTORIES SHOWN IN FIGURE 1

Quantity	Stellar Case	AGN Case
B_{00}[a]	3×10^3 G	
R_m[a]	1×10^{10}	
n_p[a]	10^{16} cm^{-3}	
B_{max}[a]	4×10^6 G	
$E_z(t_{switch}, r)$	6×10^6 cgs units	
$p_{initial}$[a]	0	
$r_{initial}/R_0$[a]	0.9	
R_0[a]	3×10^6 cm	3×10^{12} cm
Central mass[a]	$10\ M_\odot$	$10^7\ M_\odot$
r_S[a]	3×10^6 cm	3×10^{12} cm
L_B[a]	3×10^6 cm	3×10^{12} cm
Δt_{switch}	30 μs	30 s
t_0[a]	44 μs	44 s
W(eV)	4×10^{14}	4×10^{20}

[a] Input parameters chosen.

If we consider the case of a disk of density $\sim 10^{16}$ cm^{-3} around a $10^8\ M_\odot$ black hole, we find that particles may be accelerated to $\sim 10^{21}$ eV in an electromagnetic burst proceeding to $B \sim B_{collapse}$. In Table 1 our numerically computed values for AGNs with $M = 10^7\ M_\odot$ are listed. The values obtained there are not subject to the approximations adopted in the derivation of equation (31). It is likely that in the center of our Galaxy a similar mechanism may be operative but with lesser intensity: the extreme condition adopted above is replaced by $R_0 \sim r_S \gg L_B$, leading to the maximum energy lower than equation (3) by several orders of magnitude.

5. NUMERICAL WORK

Though we cannot deduce the spectrum of particle energies, we are able to calculate individual particle trajectories if the burst characteristics and the time and location of the decoupling from the MHD flow are assumed. In this section we present examples of calculated particle trajectories. These results are illustrative of the time scales, energies, and momenta expected in the explosive acceleration.

The special relativistic equations of motion were normalized and incorporated in a code using the IMSL routine DGEAR to numerically integrate the differential equations and compute the trajectories of particles under the influence of the specified forces. The fields were prescribed according to equations (15), (16), and (17) until the field evolution was cutoff. For simplicity this cutoff was enforced when the peak azimuthal magnetic field (which occurs at the edge of the explosive region) reached a preset limiting value, B_{max}. After the limit was reached, all the electromagnetic fields were set to zero and the particle was left to coast ballistically, subject only to gravitational forces. Similarly, if the particle left the region of the approximation, all electromagnetic fields were set to zero. The components of momentum in the radial and z directions were obtained by integrating equations (26) and (27). The azimuthal velocity was prescribed with regard to conservation of angular momentum. The r and z cordinates of the particles were calculated by integrating the equations $v_r = p_r/\gamma_m$ and $v_z = p_z/\gamma_m$, with γ given by

$$\gamma = \left(1 + \frac{p^2}{m^2c^2}\right)^{1/2} .$$

As noted in § 3 and 4, particles are likely to respond ballistically to the electromagnetic fields either if they are close to the null point where the MHD approximation breaks down, or if they are initially in the low-density regions at the surface of the disk. In Figure 2 we present trajectories for electrons from the low-density region at the surface of the disk. The axes are labeled with normalized units: the unit of length, $\hat{l}$, is 3×10^5 cm, the Schwarzschild radius of a 1 $M_\odot$ black hole; the unit of time is the light travel time across $\hat{l}$, 10^{-5} s; and the unit of mass is the electron mass, m_e. The zero point of the time axis corresponds to the moment at which the particle decouples

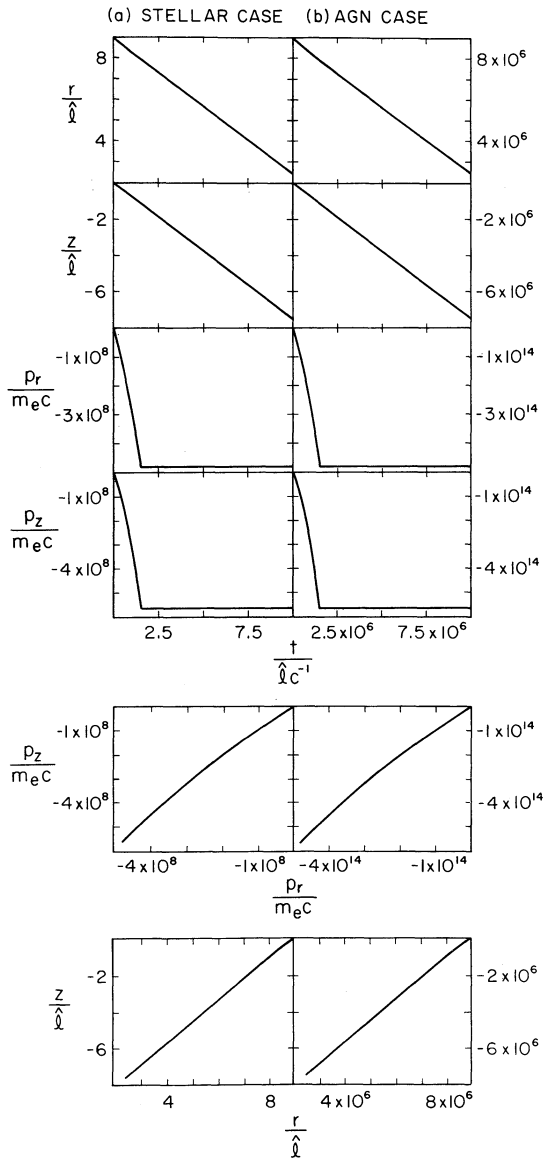

FIG. 2.—Trajectories of electrons which decouple from the MHD flow close to the edge of the explosive region a short time before the field evolution is terminated. The case of a 10 $M_\odot$ central object is shown in (*a*); in (*b*) the central object mass is $10^7\ M_\odot$. The axes are labeled in normalized units, the unit of length $\hat{l}$ is the Schwarzschild radius of a 1 $M_\odot$ black hole: 3×10^5 cm; the unit of time is the light travel time across $\hat{l}$: 1×10^{-5} s; the unit of mass is m_e. The parameters for cases (*a*) and (*b*) were scaled with respect to the Schwarzschild radius of the central object (see Table 1). The two trajectories are identical in shape.

from the MHD flow. Figure 2*a* shows a trajectory accelerated in a disk around a 10 $M_\odot$ compact object. Figure 2*b* shows the analogous trajectory for the case of a 10^7 $M_\odot$ compact object. The parameters of these two trajectories are given in Table 1. The parameters $p_{\rm initial}$ and $r_{\rm initial}$ refer to the momentum and position of the particle at the instant of decoupling; in the case of the examples given here, the particles were initially at rest in the corotating frame. The time at which the fields are switched off is indicated by $\Delta t_{\rm switch}$ $(= t_0 - t_{\rm switch})$; $E_z(t_{\rm switch}, r)$ is the electric field experienced by the particle at the instant that the field evolution is terminated. The 10 $M_\odot$ case is illustrative of an X-ray binary (e.g., SS 433) while the 10^7 $M_\odot$ case is relevant to an AGN. The spatial scales were changed to preserve their size with respect to the Schwarzschild radius, r_S, and temporal scales were changed to preserve the light travel time across r_S. The trajectories shown in Figure 2*a* and Figure 2*b* are the same shape, though, as might be expected, the energy attained by the AGN particle is increased relative to that of the SS 433 particle by the ratio of the central masses.

The limiting magnetic field, $B_{\rm max}$, in Table 1 is about a factor of 10 higher than $B_{\rm collapse}$. Such a choice may be representative of the more extreme electromagnetic bursting episodes: further explosive growth of the fields during the pressure-driven collapse could lead to $B_{\rm max} > B_{\rm collapse}$. As the limiting magnetic field increases, the burst proceeds to a smaller value of $\Delta t = t_0 - t$. The bursting fields given by equations (15), (16), and (17) increase accordingly; since the first component in E_z has the most explosive dependence on Δt, this term becomes increasingly dominant as more extreme bursts are considered. Thus as the limiting magnetic field is increased, the particles become more energetic, and more highly collimated about the z axis. Note that the present mechanism of explosive acceleration is prompt: particles are directly accelerated by the field growth.

The trajectories discussed above are for small values of t_0, corresponding to particles which decouple from the fluid flow only a short time before the explosive behavior is terminated by magnetic reconnection. Earlier, particles which "decouple" from the flow execute Lamour-like motion in the growing electromagnetic fields with a guiding center drift toward the magnetic field reversal. Such motion comprises the $\boldsymbol{E} \times \boldsymbol{B}$ fluid flow and thus these particles are not actually detached from the MHD flow, or are only weakly accelerated. In order to decouple from the fluid flow, the well-known (e.g., Sakai & Ohsawa 1987) decoupling condition $|\gamma\omega_c v_r| \ll |eE_z m^{-1}|$ must be satisfied. Here ω_c is the cyclotron frequency. As a result of the drift, when the most extreme field evolution occurs these particles are close to the field reversal, and hence are not so highly accelerated. These lower acceleration particles may provide a significant contribution to the population of the accretion disk corona. We expect highly energetically accelerated particles in a very tiny fraction of particles coming into the field null region. A typical energy spectrum in an explosive coalescence (Tajima et al. 1987) shows exponential to power-law decay as energy increases.

6. DISCUSSION OF RESULTS

We have examined electromagnetic field evolution occurring in an accretion disk. Once a seed magnetic field is supplied to the disk, flux-freezing causes a buildup of magnetic energy. Adopting the tightly wrapped, banded structure with reversals in azimuthal field direction found in the computations of Tajima & Gilden (1987), we showed how explosive solutions for the electromagnetic fields arise. When isolated plasma elements enter the asymptotically nonlinear regime, the field configuration undergoes a violent, self-driven pinching nonlinear instability. The extreme growth of the magnetic field induces correspondingly explosive electric field evolution.

The majority of the particles in the disk plasma comprise the MHD fluid and execute Lamour oscillations with a guiding center drift toward the null region. Particles which decouple from the MHD flow during the electromagnetic burst will be ballistically and promptly accelerated by the fields. A large proportion of the decoupled particles are expected to originate in the region close to the magnetic field reversal. Most such particles will experience only moderate acceleration. Some particles will, however, decouple from the fluid motion in the low-density regions at the base of the accretion disk corona. If they decouple late and the fields are intense, these particles are rapidly accelerated away from the disk. The energy of the ejected particles and the degree of collimation are dependent on the position and time at which the particle decouples, and on the limiting magnetic field of the burst. The first term in the z component of the electric field has the most explosive evolution, and hence is increasingly responsible for the particle acceleration in the most extreme bursts. This term is proportional to r^2. Thus the most extreme energies are attained by particles which originate close to the edge of the region of electric field induction, where r^2 is largest; these particles are also the most tightly collimated about the z axis. However, even particles which fall into this category are not tightly collimated: this is clear from the bottom panels of Figures 2*a* and 2*b*. From a single burst we therefore expect to obtain many low-energy particles, some of which may fail to escape the system, with the spectrum of emitted particles $n_p(E)$ decreasing as energy E increases. The interaction of the ejected charged particles, particularly electrons, with the coronal magnetic fields will lead to synchrotron emission as observed in extragalactic radio jets. Particles which are initially only weakly collimated may be entrained in the coronal magnetic fields which to first order are open and in the z direction. Particles of too low an energy to escape from the system may be an important source of the accretion disk corona population.

For the length scales involved in AGNs, and using estimates or magnetic field strength from the literature (e.g., Hughes, Allen, & Allen 1989) it is clear that synchrotron energy losses will be very significant for the ultrarelativistic particles produced by our model. Only in cases where the velocity of the particle and the magnetic field are coaligned or where the phase of the accelerating structure is synchronized with particles (the so-called "surfatron condition," Katsouleas & Dawson 1983; Sagdeev & Shapiro 1973) will the particles emerge with their initial energy undiminished by synchrotron losses. The high-energy electrons can also lose energy by inverse Compton scattering on the photons in the ambient radiation field; however, these losses are not significant compared to losses in pair-producing interactions with photons. The cross section for pair-production is given by Jauch & Rohrlich (1976); assuming an ultraviolet photon density of $n_{\rm uv} \sim 10^{14}$ cm^{-3}, this leads to a mean free path of $\sim 10^{10}$ cm for a particle of $\gamma \sim 10^{15}$. Thus, the particle will undergo many pair-producing interactions, each of which will reduce its energy. However, the dominant contribution to the cross section for these interactions comes from collisions with low momentum transfer, i.e., collisions in which the energy of the initial particle is reduced only by a small percentage. Thus, depending on the geometry and the density of the photon distribution, it is possible, though

perhaps not terribly likely, that some of the ultra–high-energy particles will emerge into the intergalactic medium. Rees (1984) speculates that in general jets may deposit their energy in the emission-line region surrounding the central accelerating engine, and only in especially favorable cases does the jet material penetrate beyond 10^{18} cm. On the other hand, since the present explosive acceleration length is short and the energy loss processes are moderate, as long as a moderate additional acceleration is provided such as the electromagnetic wave surfatron acceleration in the plasma the maintenance of some high-energy components cannot be ruled out.

A self-consistent study of the interaction of the ultrarelativistic particles discussed herein with the ambient gas and electromagnetic and radiation fields is beyond the scope of this paper, not least because the relevant parameters are highly uncertain. Rees (1984) gives a review of the processes which would need to be considered in such an undertaking. In the remainder of the paper we discuss the possible applications of this work to the problem of cosmic-ray origin.

The model discussed produces a hard, or high-energy outflow from an accretion disk as an indirect result of the liberation of gravitational energy in the region of the compact object through kinetic and electromagnetic processes. We emphasize that the acceleration is essentially prompt and impulsive and that the exploding plasma element is tiny compared to the dimensions of the disk. We have not discussed the bulk outflow present in astrophysical jets, which involves the physics of large-scale hydrodynamic flows.

It is reasonable to surmise that the characteristic spatial scale of the bursting regions is proportional to the Schwarzschild radius of the central compact object, r_S. In this case the energy of the emitted particles is proportional to the mass of the central object as shown in § 4. Thus the model predicts particles of far higher energy (and presumably more of them) from disks around AGNs than from disks around stellar mass compact objects. This has interesting implications for the production of cosmic rays. It is accepted that the bulk of cosmic rays, those with energies $\lesssim 10^{17}$ eV, have Galactic origins, and are contained by the Galactic magnetic field. From equation (31) we see that a mass of 3 $M_\odot$ for the compact object leads to particles accelerated to energies of $\sim 10^{13}$ eV. Thus our mechanism applied to magnetically catalysmic accretion disks in interacting binary star systems produces particles of energies consistent with the observed Galactic cosmic rays. On the other hand, ultra–high-energy cosmic rays with energies $\gtrsim 10^{17}$ eV apparently have extragalactic origins within the local supercluster (Strong, Wdowczyk, & Wolfendale 1974). These ultra–high-energy cosmic rays may be identified with particles accelerated from AGN systems with compact object masses $\geq 10^5\ M_\odot$.

In Table 1 examples with compact object mass of 10 $M_\odot$ and $10^7\ M_\odot$ are considered. Our results in Table 1 are derived from our numerical integration discussed in § 5 without the simplifying approximations leading to equation (31). With a mass of 10 $M_\odot$ we expect energies of $\sim 10^{15}$ eV; while with a compact object mass of $10^7\ M_\odot$, energies of $\sim 10^{21}$ eV are obtained according to these computations. Input parameters in the numerical work are indicated in Table 1. We chose parameters likely to yield the highest energy particles for a typical electromagnetic burst. However, we admit that these choices are somewhat arbitrary and different choices will lead to different highest energies.

If we consider an object such as Cygnus X-3 with a compact object mass of order 1 $M_\odot$, our computational result scales to yield highest energies of $\sim 10^{14}$ eV. It is interesting to note that this number is in the vicinity of the observed highest γ-ray energies (Samorski & Stamm 1983; Lloyd-Evans et al. 1983).

For ultra–high-energy cosmic rays Linsley (1981) discusses energies up to 10^{20} eV, and concludes that those with energies greater than 10^{19} eV are of extragalactic origin. Rochester & Turver (1981) conclude that cosmic rays of energies 10^{17}–10^{20} eV are extragalactic in origin. The latter paper discusses acceleration mechanisms: the Fermi (1949) mechanism fails to explain the observed heavy-element component of cosmic rays, while shock waves from supernovae can provide such acceleration. Shock wave acceleration is, however, probably deficient when high-energy cosmic rays are considered; though it is, however, a suitable candidate, for example, for gamma-ray ($\lesssim 10^9$ eV) bursts (Holcomb & Tajima 1991).

The interaction of high γ-particles with the cosmic background radiation leading to pair production of electron-positrons and pions has been predicted to cause the Greisen-Zatsepin cutoff in the predicted energy spectrum at $\sim 10^{19}$ eV (Strong et al. 1974). In fact, the observed ultra–high-energy spectrum of cosmic rays does not show this sharp cutoff predicted by Greisen (1966) and Zatsepin & Kuzmin (1966), but extends beyond 10^{20} eV. This can be explained if only the more energetic cosmic rays are extragalactic. Strong et al. (1974) and Linsley (1981) suggested that (i) the apparent isotropy of cosmic rays beyond 10^{18} eV indicates the extragalactic origin and (ii) some directiveness of $\sim 10^{20}$ eV components from the local supercluster direction indicates an origin within the local supercluster for this range of energies. See also Watson (1980); Stecker (1968 and 1989) discusses steady state cosmic-ray theory, addressing the local supercluster origin. For more discussion there are many recent papers in the cosmic-ray physics conference proceedings (e.g., Chudakov 1987).

Our mechanism for the production of ultrarelativistic cosmic rays with energies greater than 10^{17} eV due to particle acceleration from AGNs is consistent with the observed features as reviewed in the above: (i) the extragalactic origin; (ii) the possible local supercluster orientation for energies $\sim 10^{20}$ eV; (iii) apparent isotropy for energies $\gtrsim 10^{17}$ eV due to the many extragalactic AGN sources available. Our mechanism can produce the energies well in excess of the Greisen-Zatsepin cutoff ($\sim 10^{19}$ eV) which are required to explain the observations.

Many questions are left open. The present model does not predict the spectrum. However, the recent general theory (Mima et al. 1991) allows the generic formation of the power-law spectrum. Further, since we do not have a complete solution for the topology of the disk/boundary region magnetic field including turbulence and three-dimensional behavior, it is impossible to say what proportion of the plasma at the inner edge of the disk will be undergoing our explosive evolution at a given time. It is certain that only a small proportion of the mass in the disk will be ejected in the form of high-energy particles, since it consists only of those particles which decouple from the fluid motion and respond ballistically to the fields in a phase-synchronous fashion.

Our mechanism produces bursts of high-energy particles, rather than a continuous stream of them. The model thus predicts sporadic bursts of emission associated with the ejection of energetic charged particles. Such intermittent temporal behavior is phenomenologically analogous to the millisecond radio

spikes which occur during solar flares (Benz 1986). If the millisecond radio spikes are interpreted as a result of sporadic acceleration of particles by electric fields which detach particles from the ambient magnetic field (Tajima et al. 1990), then the origins of intermittancy in the two processes are physically analogous.

The work was supported by NSF grant ATM-91-13576, US Department of Energy DE-FG05-80ET 33088, and NASA grant NAGW-2678. C. A. H. gratefully acknowledges support from Zonta International Amelia Earhart fellowships while concluding this work. Discussions with Dr. K. Shibata, Dr. R. Lovelace, and Dr. K. Horne are appreciated.

APPENDIX A

TRANSFORMATION TO THE ROTATING FRAME

The induction equation and Euler's equation in an inertial frame are

$$\frac{\partial \boldsymbol{B}}{\partial t} = \nabla \times \boldsymbol{v} \times \boldsymbol{B} + \eta \nabla^2 \boldsymbol{B} \tag{A1}$$

$$\frac{\partial \boldsymbol{v}}{\partial t} + (\boldsymbol{v} \cdot \nabla)\boldsymbol{v} = \frac{(\nabla \times \boldsymbol{B}) \times \boldsymbol{B}}{\rho} + \nabla \Phi + \frac{\nabla \cdot \boldsymbol{t}}{\rho} . \tag{A2}$$

Here $\boldsymbol{t}$ is the viscous stress tensor. In an axisymmetric accretion disk it is a good approximation to neglect all components of $\boldsymbol{t}$ except for $t_{\theta r}$. In this case then, the viscous term becomes

$$\nu\left(\frac{\partial^2 v_\theta}{\partial r^2} + \frac{1}{r}\frac{\partial v_\theta}{\partial r}\right) . \tag{A3}$$

The viscous term is included here in Euler's equations for completeness: we neglect it in the nonlinear analysis, where linear dissipative terms are unimportant compared to the nonlinear forces which drive the explosive evolution. In order to make clearer the separation of the effects of the Keplerian velocity and those of velocity perturbations, in this paper we used a rotating frame of reference chosen to be rotating at the Keplerian velocity of the blob of plasma whose behavior we examine. The transformation of frames of reference is achieved by noting that

$$\left(\frac{\partial \boldsymbol{A}}{\partial t}\right)_{\text{inertial}} = \left(\frac{\partial \boldsymbol{A}}{\partial t}\right)_{\text{rot}} + \boldsymbol{\Omega} \times \boldsymbol{A} , \tag{A4}$$

where

$$\left(\frac{\partial}{\partial t}\right)_{\text{rot}} = \frac{\partial}{\partial t} + \omega \frac{\partial}{\partial \theta} , \tag{A5}$$

and that

$$\left(\frac{d}{dt}\right)_{\text{inertial}} = \left(\frac{\partial}{\partial t}\right) + (\boldsymbol{v} \cdot \nabla) = \left(\frac{\partial}{\partial t}\right)_{\text{rot}} + (\boldsymbol{u} \cdot \nabla) + \boldsymbol{\Omega} \times \quad . \tag{A6}$$

Here $\boldsymbol{u}$ is the velocity with respect to the rotating frame, i.e., at the radius of interest, $\boldsymbol{u}$ consists of the deviations from Keplerian motion. The electromagnetic fields and current will transform according to the Lorentz transform:

$$\boldsymbol{E} = \gamma\left(\boldsymbol{E}' - \frac{\boldsymbol{v}_0 \times \boldsymbol{B}'}{c}\right) , \tag{A7}$$

$$\boldsymbol{B} = \gamma\left(\boldsymbol{B}' - \frac{\boldsymbol{v}_0 \times \boldsymbol{E}'}{c}\right) , \tag{A8}$$

$$\boldsymbol{J} = \gamma(\boldsymbol{J}' + \rho_e \boldsymbol{v}_0) , \tag{A9}$$

where $\boldsymbol{v}_0 (= \boldsymbol{\Omega} \times \boldsymbol{r})$ is the velocity of the moving frame, and primes denote quantities defined with respect to the rotating frame. Applying this transformation to Maxwell's equations,

$$\nabla \times \boldsymbol{E} = -\frac{1}{c}\frac{\partial \boldsymbol{B}}{\partial t} , \tag{A10}$$

$$\nabla \times \boldsymbol{B} = \frac{1}{c}\frac{\partial \boldsymbol{E}}{\partial t} + \frac{4\pi \boldsymbol{J}}{c} , \tag{A11}$$

we obtain

$$\nabla \times \boldsymbol{E}' + \left[\frac{1}{c}\left(\frac{\partial}{\partial t}\right)_{\rm rot} + \frac{\boldsymbol{\Omega}}{c}\right]\left(\frac{\boldsymbol{v}_0 \times \boldsymbol{B}'}{c}\right) = -\frac{1}{c}\left(\frac{\partial}{\partial t}\right)_{\rm rot}\boldsymbol{B}' + \frac{\boldsymbol{\Omega} \times \boldsymbol{B}'}{c} + \nabla \times \left(\frac{\boldsymbol{v}_0 \times \boldsymbol{B}'}{c}\right), \tag{A12}$$

$$\nabla \times \boldsymbol{B}' + \left[\frac{1}{c}\left(\frac{\partial}{\partial t}\right)_{\rm rot} + \frac{\boldsymbol{\Omega}}{c}\right]\left(\frac{\boldsymbol{v}_0 \times \boldsymbol{E}'}{c}\right) = -\frac{1}{c}\left(\frac{\partial}{\partial t}\right)_{\rm rot}\boldsymbol{E}' + \frac{\boldsymbol{\Omega} \times \boldsymbol{E}'}{c} + \nabla \times \left(\frac{\boldsymbol{v}_0 \times \boldsymbol{E}'}{c}\right). \tag{A13}$$

As a simplifying approximation we treat the disk as axisymmetric, so that terms involving $\partial/\partial\theta$ are zero, so that $(\partial/\partial t)_{\rm rot}$ can simply be replaced by $\partial/\partial t$.

We may make use of Ohm's law to express $\boldsymbol{E}'$ in terms of $\boldsymbol{B}'$. In the inertial frame we have

$$\boldsymbol{E} = -\frac{\boldsymbol{v} \times \boldsymbol{B}}{c} + \eta \boldsymbol{J}\,. \tag{A14}$$

Transforming and collecting terms this becomes

$$\left[1 - \left(\frac{\boldsymbol{u} \times \boldsymbol{v}_0}{c^2}\right)\times\right]\boldsymbol{E}' = -\frac{\boldsymbol{u}}{c} \times \boldsymbol{B} + \eta(\boldsymbol{J}' + \rho_e \boldsymbol{v}_0)\,, \tag{A15}$$

In the nonrelativistic regime we may neglect terms of order u/c or v/c. So we have

$$\boldsymbol{E}' = \frac{\boldsymbol{u} \times \boldsymbol{B}'}{c} + \eta \boldsymbol{J}'\,, \tag{A16}$$

$$\boldsymbol{j}'' = (\boldsymbol{J}' + \rho_e \boldsymbol{v}_0)\,, \tag{A17}$$

and substituting for $\boldsymbol{E}'$ in the nonrelativistic versions of equations (A12) and (A13) yields

$$\frac{\partial \boldsymbol{B}'}{\partial t} + \boldsymbol{\Omega} \times \boldsymbol{B}' - \nabla \times (\boldsymbol{u} + \boldsymbol{v}_0) \times \boldsymbol{B}' = \eta c \nabla \times \boldsymbol{j}'\,, \tag{A18}$$

$$c\nabla \times \boldsymbol{B}' = -\eta \nabla \times \boldsymbol{v}_0 \times \boldsymbol{j}' + 4\pi \boldsymbol{j}' + \eta\left(\frac{\partial}{\partial t} + \boldsymbol{\Omega}\times\right)\boldsymbol{j}'\,. \tag{A19}$$

Since $\boldsymbol{v}_0$ is azimuthal and $\boldsymbol{B}'$ is predominantly azimuthal, $\boldsymbol{v}_0 \times \boldsymbol{B}'$ is very small compared to $\nabla \times \boldsymbol{B}$ and may therefore be neglected in comparison to the other terms. We now need to express the current $\boldsymbol{j}''$ in terms of $\boldsymbol{B}$. Assuming that the plasma is highly conducting, the resistivity, η, is small; hence the first and third terms on the right-hand side of equation (A19) can be neglected. Thus we have

$$c\nabla \times \boldsymbol{B}' = 4\pi \boldsymbol{j}'\,. \tag{A20}$$

Substituting for $\boldsymbol{j}''$ in equation (A18), we obtain the induction equation in the rotating frame of reference

$$\frac{\partial \boldsymbol{B}'}{\partial t} + \boldsymbol{\Omega} \times \boldsymbol{B} - \nabla \times (\boldsymbol{u} \times \boldsymbol{B}) = \frac{c^2 \eta}{4\pi} \nabla \times (\nabla \times \boldsymbol{B})\,. \tag{A21}$$

We also need to transform Euler's equation. The left-hand side transforms according to

$$\left(\frac{d^2 \boldsymbol{r}}{dt^2}\right)_{\rm inertial} = \left(\frac{d^2 \boldsymbol{r}}{dt^2}\right)_{\rm rot} + 2\boldsymbol{\Omega} \times \boldsymbol{u} + \boldsymbol{\Omega} \times (\boldsymbol{\Omega} \times \boldsymbol{r})\,, \tag{A22}$$

where $\boldsymbol{u} = (d\boldsymbol{r}/dt)_{\rm rot}$ as before. So transforming the current and magnetic field as before and making use of the conditions $\eta \ll 1$, and $v/c \ll 1$ and dropping the primes, since all quantities henceforth are in the rotating frame, we obtain

$$\frac{\partial \boldsymbol{u}}{\partial t} + (\boldsymbol{u} \cdot \nabla)\boldsymbol{u} + 2\boldsymbol{\Omega} \times \boldsymbol{u} = \boldsymbol{j}'' \times \boldsymbol{B} + \frac{\nabla \cdot \boldsymbol{t}}{\rho}\,. \tag{A23}$$

Using equation (A20) to substitute for $\boldsymbol{j}'$, the Euler equation in the rotating frame becomes

$$\frac{\partial \boldsymbol{u}}{\partial t} + (\boldsymbol{u} \cdot \nabla)\boldsymbol{u} + 2\boldsymbol{\Omega} \times \boldsymbol{u} = \frac{c}{4\pi}(\nabla \times \boldsymbol{B}) \times \boldsymbol{B}\,. \tag{A24}$$

APPENDIX B

THE EINSTEIN-LIKE RELATIONSHIP BETWEEN VISCOSITY AND MOBILITY IN TURBULENT MAGNETIC PLASMAS

In this Appendix we present a result which emerged during our discussions of accretion disk magnetic field structure.

In the nonmagnetic, classical, collisional plasma, the relationship between the viscosity and the mobility is embodied in the well-known Einstein relation (Einstein 1905)

$$\frac{\mu}{D} = \frac{e}{kT_e}, \tag{B1}$$

where we are using μ for the mobility,

$$\mu = \frac{\sigma}{ne}, \tag{B2}$$

σ is the conductivity, and D is the electron diffusion coefficient:

$$D = \frac{kT_e}{m_e \nu_e}. \tag{B3}$$

In the classical magnetic case, however, this relationship changes, since the viscosity and hence the diffusion coefficient are affected by the presence of the magnetic field. In this discussion we include only the ion-ion viscosity since the electron-ion viscosity is smaller by a factor of

$$\left(\frac{M_{\rm ion}}{m_e}\right)^{-1/2}.$$

Braginskii (1985) gives both the ion viscosity perpendicular to the field:

$$\eta_{\rm vis} = \frac{0.3nkT_i}{\omega_{ci}^2 \tau_i}, \tag{B4}$$

and the conductivity perpendicular to the magnetic field:

$$\sigma_{\rm perp} = \frac{ne^2}{m_e \nu_e}. \tag{B5}$$

The viscosity and the diffusion coefficient are related by definition

$$D = \frac{\eta_{\rm vis}}{\rho} \tag{B6}$$

(where ρ is the mass density) so in this case the ratio of the mobility to the diffusion coefficient is

$$\frac{\mu}{D} = \frac{1}{2}\omega_{\rm ce}^2 \tau_e^2 \frac{e}{kT}. \tag{B7}$$

Hence we see that in the classical magnetic regime the ratio μ/D is a function of magnetic field strength: that is to say that Einstein's relation per se no longer holds. This equation reflects the change in the viscosity, which, in the classical treatment, is caused by the presence of a magnetic field.

In the case of strongly turbulent magnetic plasmas, which likely correspond to many astrophysical situations, one might expect Einstein's relation to hold, since turbulence will enhance the effective collisionality. Indeed, in the case of anomalous diffusion, this may be self-consistently assumed, as we shall show below.

Consider, for example, Bohm's formula (Bohm, Burhop, & Massey 1949) for the diffusion coefficient,

$$D_{\rm Bohm} = \frac{ckT}{16eB}, \tag{B8}$$

then in the anomalous magnetic case the viscosity is

$$\eta_{\rm vis} = \frac{nMckT}{16eB}. \tag{B9}$$

Ichimaru (1973) derived an expression for the conductivity perpendicular to the field in a turbulent magnetic plasma, in which the level of fluctuations causes a turbulent collision frequency of order $\omega_{\rm pe}$

$$\sigma = \frac{\omega_{\rm pe}^2}{\omega_{\rm ce}} \frac{\sqrt{2}}{64\pi^2} \ln\left(\frac{M_i}{m_e}\right)\left[1 + \frac{2}{(16\pi)^2}\ln^2\left(\frac{M_i}{m_e}\right)\right]^{-1}. \tag{B10}$$

Evaluating the constants for hydrogen

$$\sigma = 1.6 \times 10^{-2} \frac{\omega_{pe}^2}{\omega_{ce}}, \tag{B11}$$

$$= 1.6 \times 10^{-2} \frac{4\pi nec}{B}. \tag{B12}$$

So evaluating the ratio of the mobility to the diffusion coefficient, we find

$$\frac{\sigma/ne}{D} = 1.6 \times 10^{-2} \frac{64\pi e}{kT_e}, \tag{B13}$$

$$= 3.24 \frac{e}{kT_e}. \tag{B14}$$

Which means that when anomalous effects are considered we retrieve the same functional dependence for this ratio as the classical nonmagnetic treatment, equation (B1), yields. Equations (B1) and (B13) differ only in the numerical constant of proportionality.

REFERENCES

Begelman, M. C., Blandford, R. D., & Rees, M. J. 1984, Rev. Mod. Phys., 56, 255
Benz, A. O. 1986, Sol. Phys., 104, 99
Bohm, D., Burhop, E. H. S., & Massey, H. S. W. 1949, in The Characteristics of Electrical Discharges in Magnetic Fields, ed. A. Guthrie & R. K. Wakerling (New York: McGraw-Hill), 13
Braginskii, S. I. 1965, in Rev. Plasma Phys., 1, 205
Bridle, A. H., & Perley, R. A. 1984, ARA&A, 22, 319
Chudakov, A. E. 1987, in 20th Internat., Cosmic Ray Conf., Moscow, 6, 494
Einstein, A. 1905, Ann. d. Phys., 17, 549
Fermi, E. 1949, Phys. Rev., 75, 1169
Fujimoto, M., & Sawa, T. 1987, PASJ, 39, 375
Greisen, K. 1966, Phys. Rev. Lett., 16, 748
Holcomb, K., & Tajima, T. 1991, ApJ, 378, 682
Horne, K., Wood, J. H., & Stiening, R. F. 1991, ApJ, 378, 271
Hughes, P. A., Allen, H. D., & Allen, M. F. 1989, ApJ, 341, 68
Ichimaru, S. 1973, Basic Principles of Plasma Physics, A Statistical Approach (Reading: Benjamin)
Jauch, J. M., & Rohrlich, F. 1976, The Theory of Photons and Electrons (Berlin: Springer), 378
Kaisig, M., & Spruit, H. C. 1991, in preparation
Katsouleas, T., & Dawson, J. M. 1983, Phys. Rev. Lett., 51, 392
Linsley, J. 1981, in Origin of Cosmic Rays, ed. G. Setti, G. Spada, & A. W. Wolfendale (Dordrecht: Reidel), 53
Lloyd-Evans, J., Coy, R. N., Lambert, A., Lapikens, J., Patel, M., Reid, R. J. O., & Watson, A. A. 1983, Nature, 305, 784
Margon, B. 1984, ARA&A, 22, 507
Mima, K., Horton, W., Tajima, T., & Hasegawa, A. 1991, in Nonlinear Dynamics and Particle Acceleration, ed. Y. H. Ichikawa & T. Tajima (New York: AIP), 27
Parker, E. N. 1970, ApJ, 162, 665
Perkins, F. W., & Zweibel, E. 1987, Phys. Fluids, 30, 1079
Rees, M. J. 1984, ARA&A, 22, 471
Rochester, G. D., & Turver, K. E. 1981, Contemp. Phys., 22, 425
Sagdeev, R. Z., & Shapiro, V. P. 1973, JETP Lett., 17, 279
Sakai, J.-I., & Ohsawa, Y. 1987, Space Sci. Rev., 46, 113
Samorski, M., & Stamm, W. 1983, ApJ, 268, L17
Sawa, T., & Fujimoto, F. 1986, PASJ, 38, 133
Shibata, K., Tajima, T., & Matsumoto, R. 1990, ApJ, 350, 295
Sofue, Y., Fujimoto, M., & Wielebinski, R. 1986, ARA&A, 24, 459
Stecker, F. W. 1968, Phys. Rev. Lett., 21, 1016
———. 1989, Nature, 342, 401
Steinolfson, R. S., & Tajima, T. 1987, ApJ, 323, 503
Strong, A. W., Wdowczyk, J., & Wolfendale, A. W. 1974, J. Phys. A, 7, 1767
Tajima, T., Benz, A. O., Thaker, M., & Leboeuf, J. N. 1990, ApJ, 353, 666
Tajima, T., & Gilden, D. 1987, ApJ, 320, 741
Tajima, T., & Sakai, J.-I. 1989a, Fizika Plazmy 15, 899
———. 1989b, Fizika Plazmy 15, 1045
Tajima, T., Sakai, J.-I. Nakajima, H., Kosugi, T., Brunel, F., & Kundu, M. R. 1987, ApJ, 321, 1031
Watson, A. A. 1980, Quart. J. Roy. Astr. Soc., 21, 1
Zatsepin, G. T., & Kuzmin, V. A. 1966, JETP Lett., 4, 78